SUPPLEMENTAL MATERIAL

Deficiency of HIF1alpha in dendritic cells aggravates atherosclerosis and type 1 T helper cell responses in mice

Sweena M. Chaudhari, Judith C. Sluimer, Miriam Koch, Thomas L. Theelen, Helga D. Manthey, Martin Busch, Celia Caballero-Franco, Frederick Vogel, Clement Cochain, Jaroslav Pelisek, Mat J. Daemen, Manfred Lutz, Agnes Görlach, Stephan Kissler, Heike M. Hermanns, Alma Zernecke

Supplementary Figures and Figure Legends
Figure SI

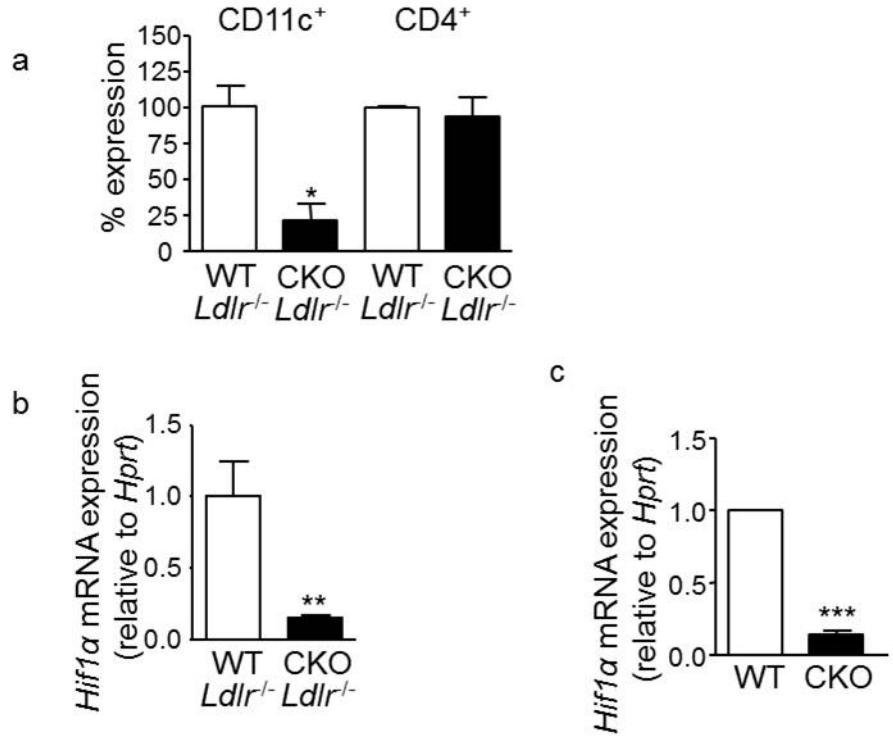

Figure SI. Hif1a deletion efficiency
(a,b) CD11c$^+$ APCs and CD4$^+$ T cells were isolated from spleens of atherosclerotic *Hif1a*-WT *Ldlr*$^{-/-}$ and *Hif1a*-CKO *Ldlr*$^{-/-}$ mice, and *Hif1a* deletion from genomic DNA (a) and *Hif1a* mRNA expression (b) was analyzed by qPCR. mRNA expression was normalized to *Hprt* reference gene and relative to WT controls (n=3 mice). (c) *Hif1a* mRNA expression was also analyzed in *Hif1a*-WT and *Hif1a*-CKO BMDCs by qPCR (n=3 mice). mRNA expression was normalized to *Hprt* and presented relative to WT controls. Data are presented as mean ± SEM. *p<0.05, ***p<0.001.

Figure SII

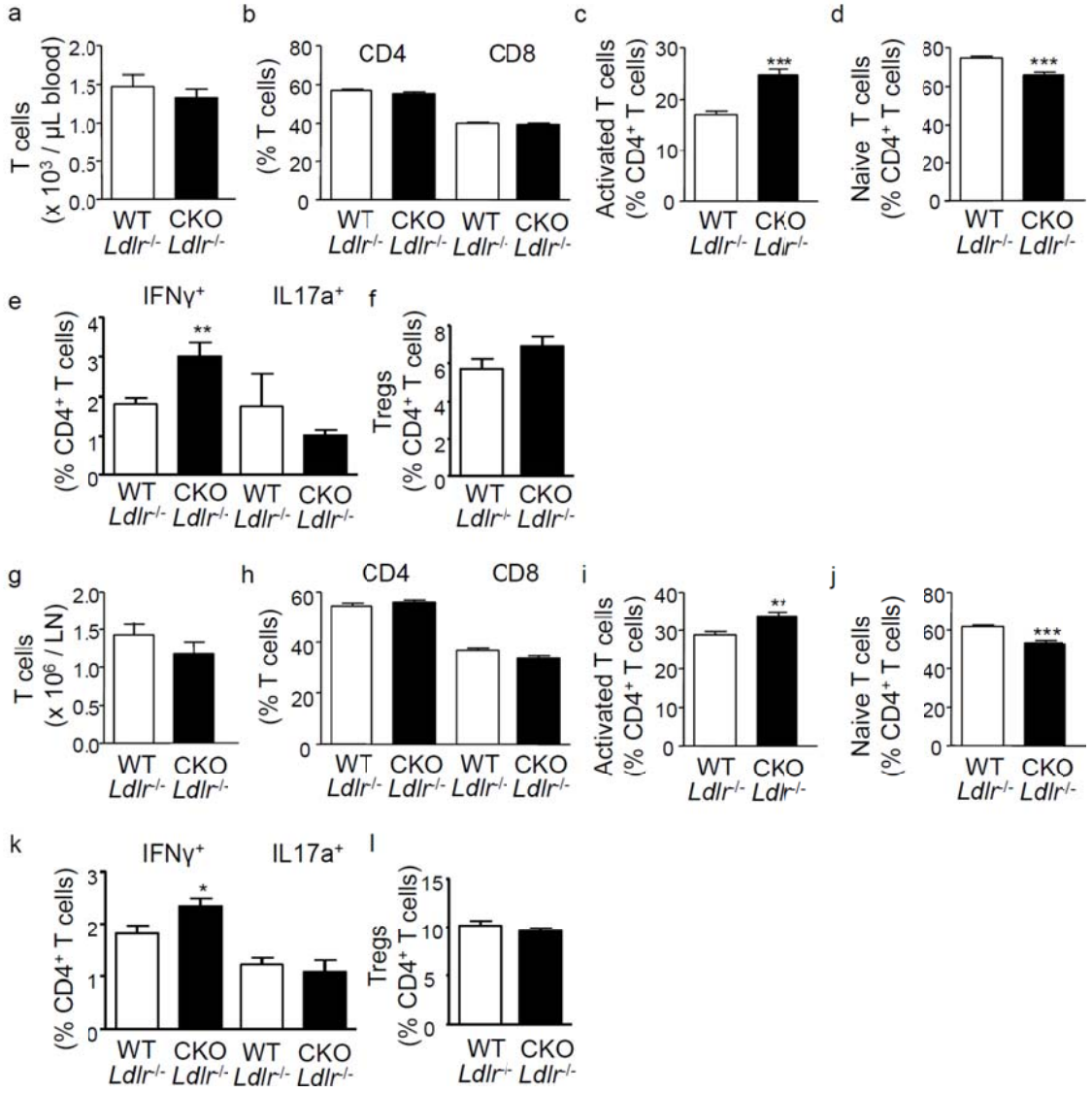

Figure SII. *Ldlr*$^{-/-}$ mice deficient in *Hif1a* in APCs display enhanced T-cell activation.
(a-l) Flow cytometric analyses of T cell distributions in blood (a-f) and lymph nodes (g-l) of atherosclerotic *Hif1a*-WT *Ldlr*$^{-/-}$ (n=10) and *Hif1a*-CKO *Ldlr*$^{-/-}$ (n=7-12) mice fed a high fat diet for 8 weeks. Numbers of $CD3^+$ T cells (a,g), frequencies of $CD4^+$ and $CD8^+$ T cells among $CD3^+$ T cells (b,h), frequencies of activated $CD44^{high}$ $CD62L^{low}$ (c,i) and naïve $CD62L^{high}$ $CD44^{low}$ $CD4^+$ T cells (d,j), IFNγ$^+$ $CD4^+$ T cells and IL-17a$^+$ $CD4^+$ T cells (e,k) and $FoxP3^+$ $CD25^+$ $CD4^+$ Tregs (f,l) were quantified. Data are presented as mean ± SEM. *p<0.05, **p<0.01, ***p<0.001.

Figure SIII.

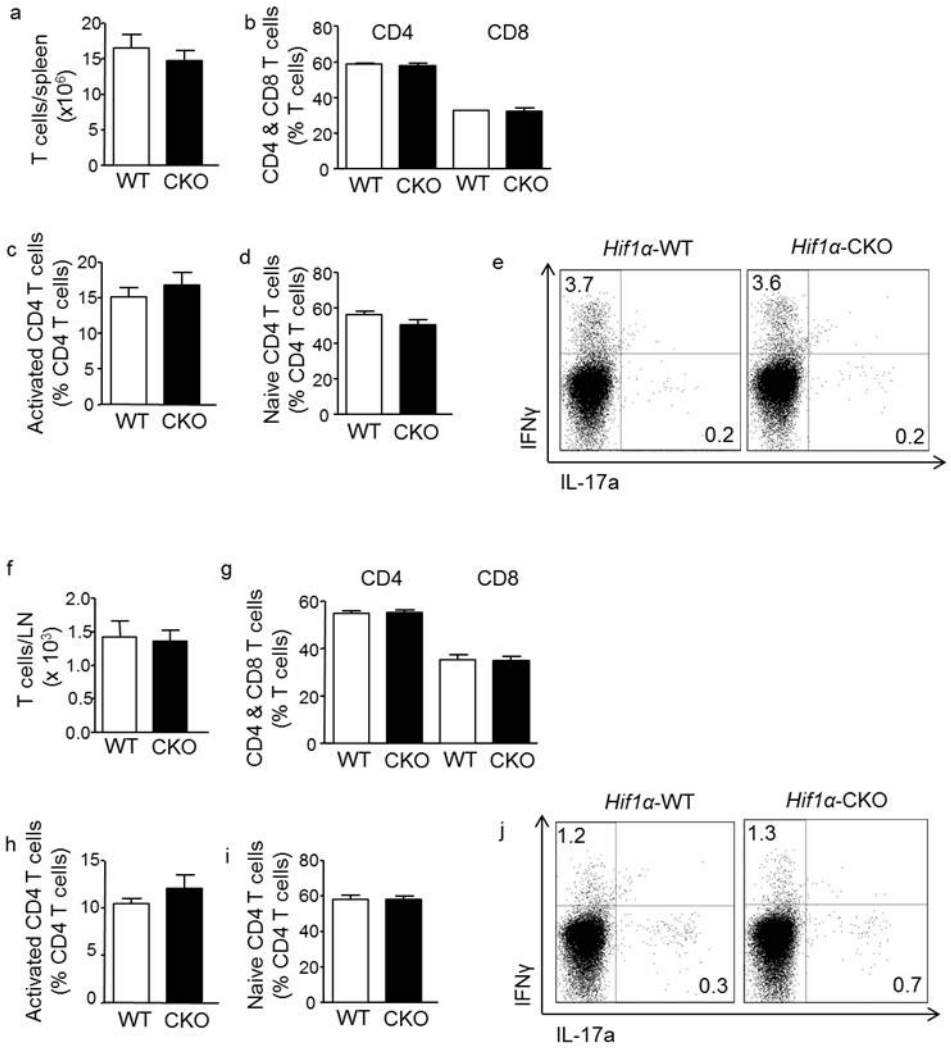

Figure SIII. Deficiency of HIF1α in APCs does not alter T-cell activation under homeostatic conditions.

(a-j) Flow cytometric analyses of T-cell distributions in spleen (a-e) and lymph nodes (f-j) of 8 week old *Hif1a*-WT (n=4 and *Hif1a*-CKO (n=4 mice). Numbers of $CD3^+$ T cells (a,f), frequencies of $CD4^+$ and $CD8^+$ T cells among $CD3^+$ T cells (b,g), frequencies of activated $CD44^{high}$ $CD62L^{low}$ (c,h) and naïve $CD62L^{high}$ $CD44^{low}$ $CD4^+$ T cells (d,i), $IFN\gamma^+$ $CD4^+$ T cells and $IL\text{-}17a^+$ $CD4^+$ T cells (e,j) were quantitated. Representative dot plots showing intracellular IFNγ versus IL-17a expression are shown; values indicate gated events among $CD4^+$ T cells. Data are presented as mean ± SEM.

Figure SIV

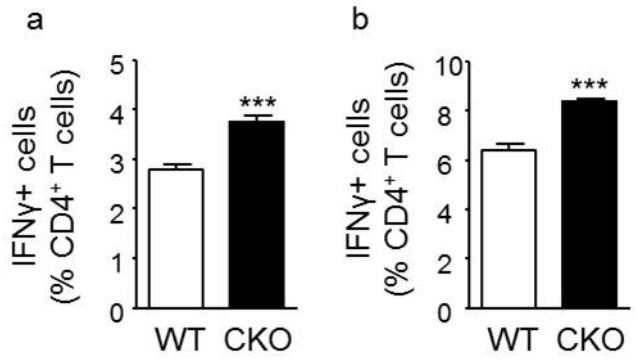

Figure SIV. Mice with HIF1α deficient APCs show enhanced Th1 polarization in response to systemic immunization

WT and CKO mice were immunized with OVA protein and CFA, and Th1 polarization was analyzed by intracellular staining for IFNγ by flow cytometry in lymph nodes (a) and spleens (b) (n=4 per group). Data are presented as mean ± SEM. ***p<0.001.

Figure SV

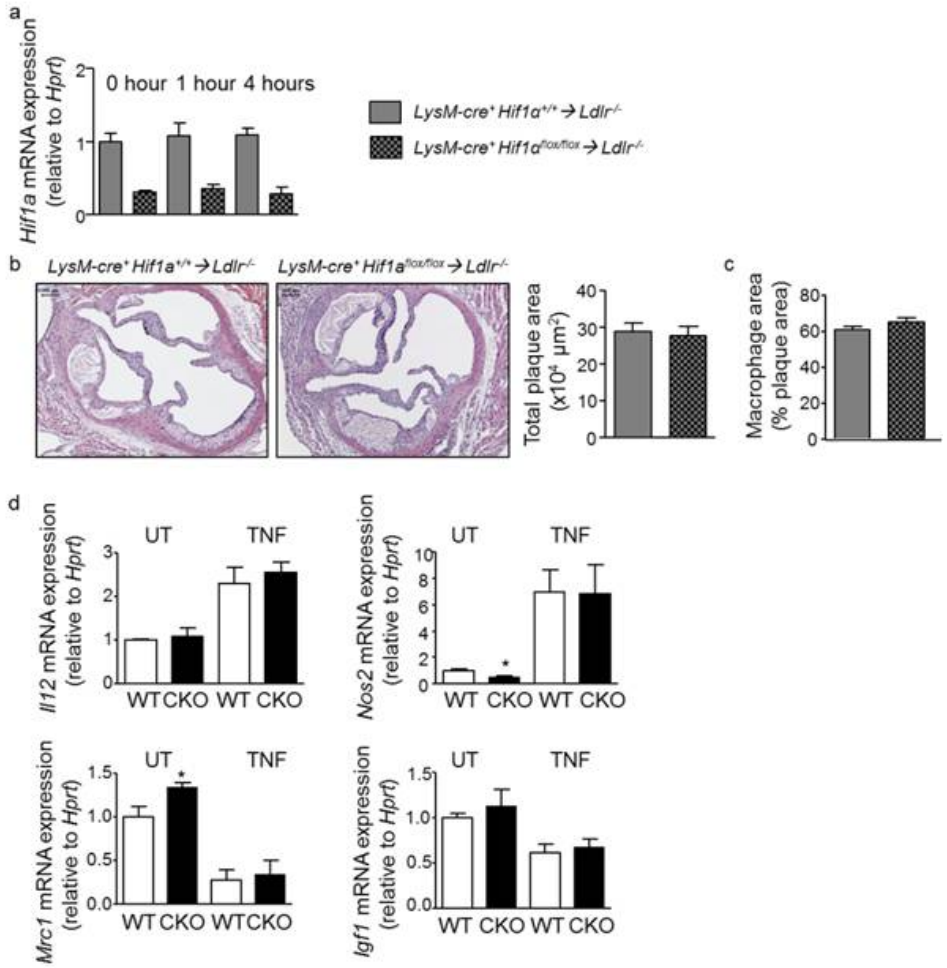

Figure SV. Deficiency of HIF1α in LysM$^+$ myeloid cells does not affect plaque growth
(a) *Hif1a* mRNA expression in bone-marrow derived macrophages from *LysM-cre$^+$Hif1a$^{+/+}$→Ldlr$^{-/-}$* mice and *LysM-cre$^+$Hif1a$^{flox/flox}$→Ldlr$^{-/-}$* mice in normoxia (0 hour) and under hypoxic conditions (0.2% O_2) for 1 and 4 hours; mRNA expression was presented relative to WT controls. (n=3 per group). (c) Quantification of plaque area and (d) plaque Mac3$^+$ macrophage content in aortic roots of atherosclerotic *LysM-cre$^+$Hif1a$^{+/+}$→Ldlr$^{-/-}$* and *LysM-cre$^+$Hif1a$^{flox/flox}$→Ldlr$^{-/-}$* mice (n=16 each) fed a high fat diet for 6 weeks; representative H&E stained sections are shown (scale bars: 100µm). (e) mRNA expression of M1 markers *Il12* and *Nos2* and M2 markers *Mrc1* and *Igf1* in untreated (UT) or TNFα (TNF) treated BMMs from *Hif1a*-CKO mice and *Hif1a*-WT mice, as assessed by qPCR. mRNA expression was normalized to *Hprt* and presented relative to *Hif1α*-WT controls (n=5). Data are presented as mean ± SEM. *p<0.05.

ifn

Figure SVI

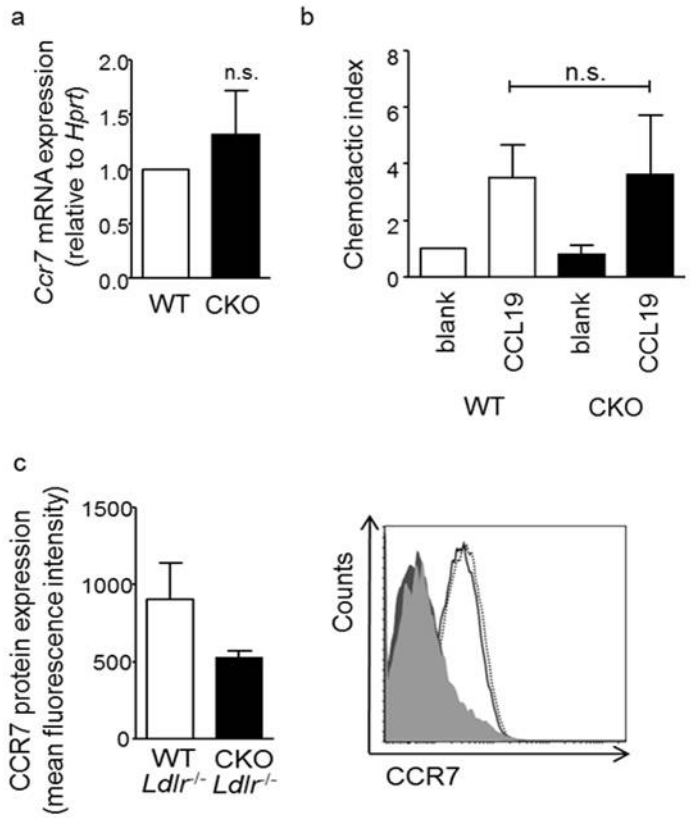

Figure SVI. *Hif1a*-deficient APCs show no alterations in CCR7 expression or migration capacity.
(a) *Ccr7* mRNA expression in BMDCs from *Hif1a*-WT and *Hif1a*-CKO mice, analyzed by qPCR (n=5 mice per group). mRNA expression was normalized to *Hprt* and presented relative to controls. (b) Migration of BMDCs from *Hif1a*-WT and *Hif1a*-CKO mice towards CCL19, as assessed in *in vitro* migration assays. Values are expressed relative to the random migration of WT BMDCs without chemotactic stimulation (blank, n=3 independent experiments, performed in triplicates). (c) CCR7 protein expression on splenic APCs from *Hif1a*-WT *Ldlr*$^{-/-}$ and *Hif1a*-CKO *Ldlr*$^{-/-}$ mice fed a high fat diet for 8 weeks (n=6 mice per group). Representative histograms depicting CCR7 expression in *Hif1a*-WT *Ldlr*$^{-/-}$ and *Hif1a*-CKO *Ldlr*$^{-/-}$ splenic APCs (solid line - *Hif1a*-WT *Ldlr*$^{-/-}$, dotted line - *Hif1a*-CKO *Ldlr*$^{-/-}$, filled dark grey line - *Hif1a*-WT *Ldlr*$^{-/-}$ FMO, filled faint grey line - *Hif1a*-CKO *Ldlr*$^{-/-}$ FMO). Data are presented as mean ± SEM.

Figure SVII.

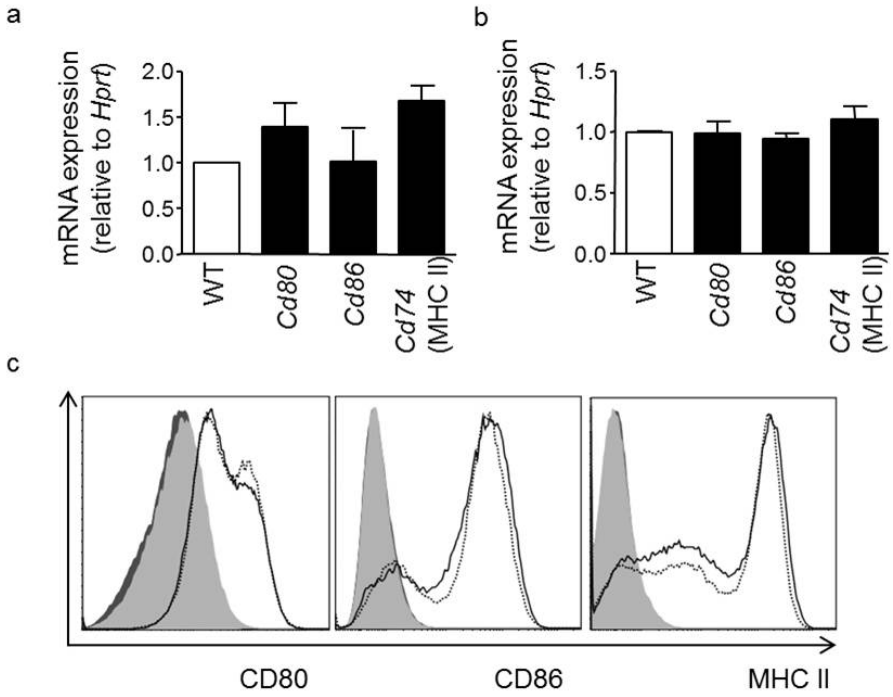

Figure SVII. Cytokine and co-stimulatory molecule expression in *Hif1a*-deficient APCs. (a) mRNA expression of indicated co-stimulatory molecules in mature BMDCs (n=3 mice) generated from *Hif1a*-WT and *Hif1a*-CKO mice and in (b) APCs isolated from spleens of *Hif1a*-WT *Ldlr*$^{-/-}$ and *Hif1a*-CKO *Ldlr*$^{-/-}$ mice fed a high fat diet for 8 weeks (n=12 mice), as analyzed by qPCR. mRNA expression was normalized to *Hprt* and presented relative to *Hif1a*-WT controls. (c) Representative histogram depicting co-stimulatory molecule expression in *Hif1a*-WT and *Hif1a*-CKO BMDCs (solid line - *Hif1a*-WT, dotted line - *Hif1a*-CKO, filled dark grey line - *Hif1a*-WT FMO, filled faint grey line - *Hif1a*-CKO-FMO). Data are presented as mean ± SEM.

Figure SVIII

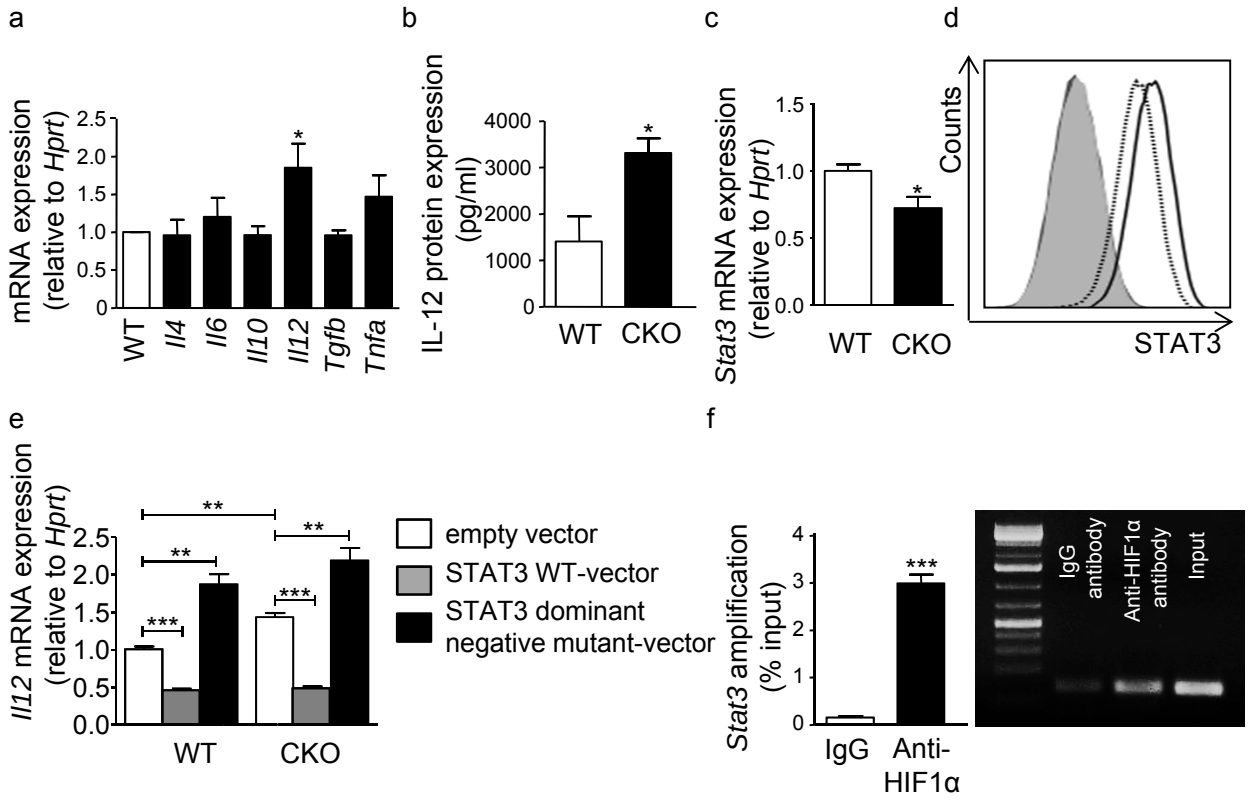

Figure SVIII. HIF1α-deficient BMDCs display increased IL-12 and decreased STAT3 expression.

(a) mRNA expression of indicated cytokines, assessed by qPCR (3 independent experiments, n=3-4 mice per experiment), (b) IL-12 protein levels in culture supernatants determined by ELISA (n=3 mice each), (c) *Stat3* mRNA expression assessed by qPCR (n=5 mice) and (d) STAT3 intracellular protein expression (n=4 mice) analyzed by flow cytometry in TNFα-matured BMDCs generated from *Hif1a*-WT and *Hif1a*-CKO mice. mRNA expression was normalized to *Hprt* and presented relative to WT controls. Representative histograms for STAT3 fluorescence are shown (solid line - *Hif1a*-WT, dotted line - *Hif1a*-CKO, filled dark grey line - *Hif1a*-WT fluorescence minus one control (FMO), filled faint grey line *Hif1a*- CKO FMO). (e) *Il12* mRNA expression in *Hif1a*-WT and *Hif1a*-CKO BMDCs transfected with pCAGGS-STAT3 wild type vector, pCAGGS-STAT3D dominant negative mutant vector, or empty vector, analyzed by qPCR (normalized to *Hprt* and expressed relative to *Hif1a*-WT empty vector, 3 independent experiments, n=3 mice per experiment). (f) ChIP assay was performed using anti-HIF1α antibody or respective IgG control antibody for HIF1α precipitation from C57BL/6J BMDCs. Immunoprecipitated chromatin was analyzed by qPCR using primers to HIF1α binding-sites on the *Stat3* promoter. Results were normalized to input chromatin (representative with n=3 mice from 2 independent experiments); a representative agarose gel of PCR-amplified samples is shown. *p<0.05, **p<0.01, ***p<0.001.

Figure SIX.

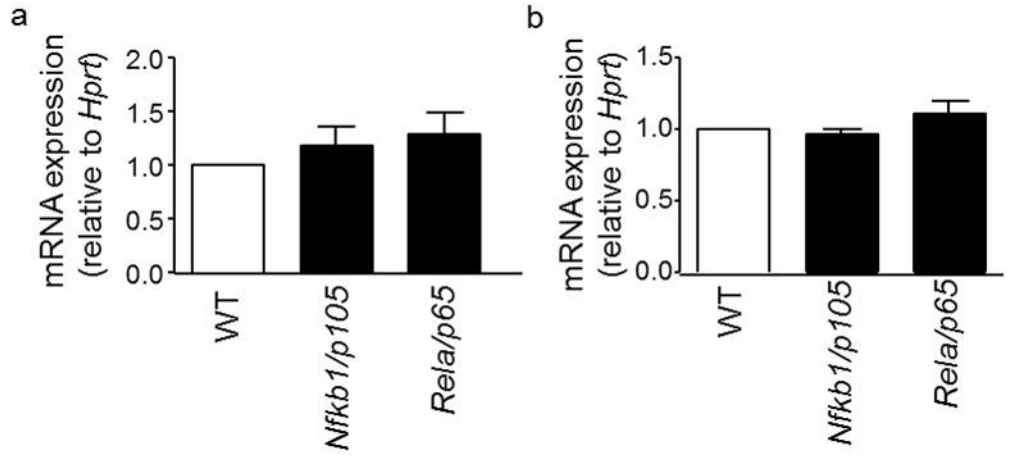

Figure SIX. *Hif1a*-deficient APCs show no changes in *Nfkb* expression.
qPCR was performed to analyze mRNA expression of *Nfkb1/p105* and *Rela/p65* in (a) mature BMDCs from *Hif1a*-WT and *Hif1a*-CKO mice (n=3 mice) and (b) splenic APCs isolated from *Hif1a*-WT *Ldlr*$^{-/-}$ and *Hif1a*-CKO *Ldlr*$^{-/-}$ mice fed a high fat diet for 8 weeks (n=12 mice). mRNA expression was normalized to *Hprt* and presented relative to controls. Data are presented as mean ± SEM.

Figure SX.

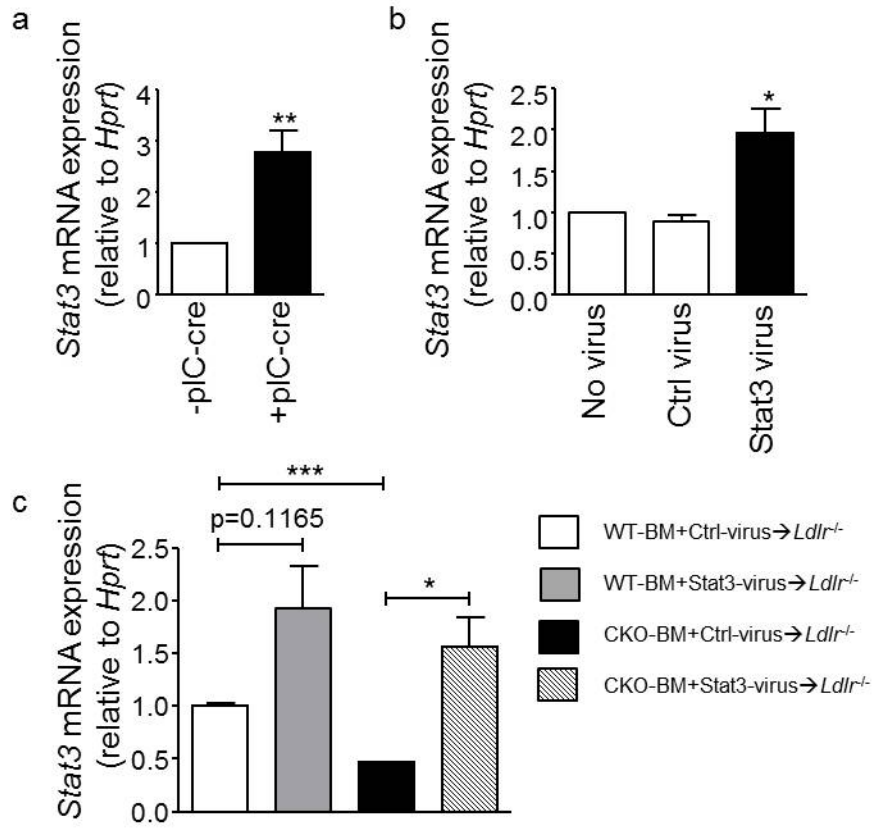

Figure SX. CD11c-specific *Stat3* mRNA expression
(a-c) qPCR analysis of *Stat3* mRNA expression in (a) HEK293F cells co-transfected with the STAT3 overexpressing vector pLB2-Ubi-FLIP-STAT3 and with or without a Cre producing pIC-cre vector (n=6 each), (b) BMDCs differentiated from BM of *Cd11c*-cre^{+} mice transduced with control or pLB2-Ubi-FLIP-STAT3 lentivirus (n=3 each) and (c) splenic APCs isolated from WT-BM+Ctrl-virus→*Ldlr*$^{-/-}$ mice, WT-BM+STAT3-virus→*Ldlr*$^{-/-}$ mice, CKO-BM+Ctrl-virus→*Ldlr*$^{-/-}$ mice and CKO-BM+STAT3-virus→*Ldlr*$^{-/-}$ mice (n=5-8 each). mRNA expression was normalized to *Hprt* and presented relative to controls. Data are presented as mean ± SEM. *p<0.05, **p<0.01, ***p<0.001.

Figure SXI.

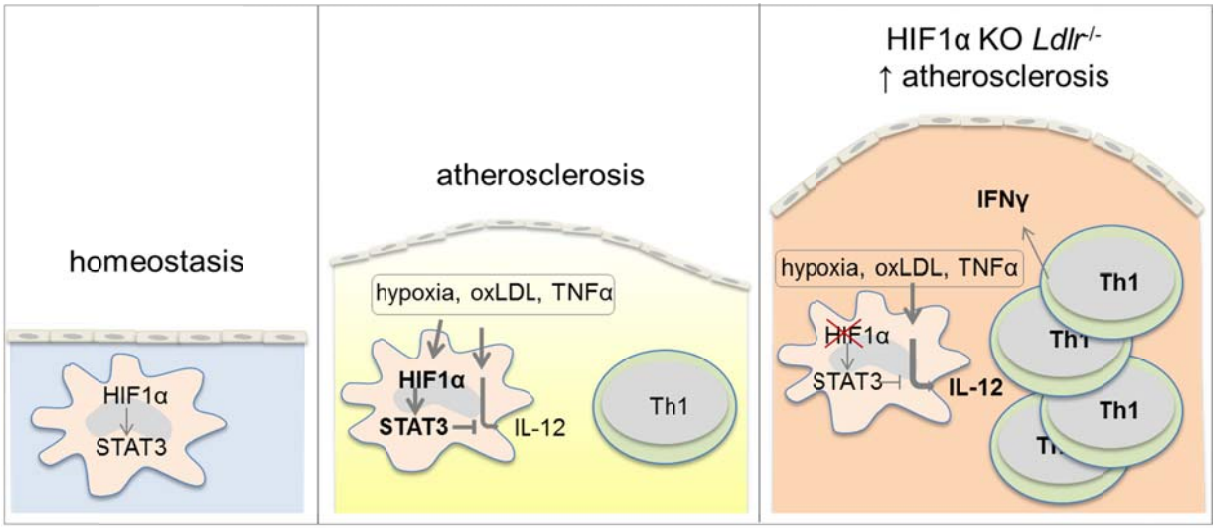

Figure SXI. Summary of main findings.
The transcription factor HIF1α is upregulated in atherosclerotic lesions in response to hypoxia or inflammatory stimuli. HIF1α directly binds the *Stat3* promotor to control its transcription. STAT3 in turn dampens pro-inflammatory IL-12 secretion, which triggers Th1 T cell activation. In CKO mice with a deletion of *Hif1a* in $CD11c^{+}$ APCs in $Ldlr^{-/-}$ mice, STAT3 expression is decreased, whereas IL-12 expression is increased, promoting an expansion of pro-inflammatory Th1 T cells and an accelerated atherosclerotic lesion formation. HIF1α thus functions to balance APC-activation and Th1-polarization during atherogenesis in $Ldlr^{-/-}$ mice, and to attenuate the progression of atherosclerosis.

Supplementary Table SI
Cholesterol levels and T cell distributions in atherosclerotic *Ldlr*$^{-/-}$(*LysM*-cre^{+}*Hif1*$\alpha^{flox/flox}$ BM) mice.

		LysM-cre^{+}*Hifa*$^{+/+}$ → *Ldlr*$^{-/-}$	*LysM*-cre^{+}*Hifa*$^{flox/flox}$ → *Ldlr*$^{-/-}$
Serum cholesterol (µg/ml)		9,384 ± 498	8,964 ± 353
Lymph nodes	$CD4^{+}$:$CD8^{+}$	0.62 ± 0.06	0.60 ± 0.05
	%$CD4^{+}CD25^{+}$	2.72 ± 0.13	2.74 ± 0.22
	%$CD3^{+}CD69^{+}$	33.16 ± 0.83	36.18 ± 0.80
Spleen	%$CD4^{+}$/$CD8^{+}$	1.00 ± 0.09	1.27 ±0.11
	%$CD4^{+}CD25^{+}$	1.44 ± 0.05	1.55 ±0.10
	%$CD3^{+}CD69^{+}$	24.72 ± 0.42	26.66 ± 1.52